At the crossroad between invariant manifolds and the role of noise

A. Guillamon

Departament de Matemàtiques, Universitat Politècnica de Catalunya, Barcelona

UNIVERSITAT POLITÈCNICA DE CATALUNYA
BARCELONATECH

Collaborators:
Oriol Castejón, Amadeu Delshams and Gemma Huguet (UPC)

Brain Dynamics and Statistics: Simulation versus Data
Banff, Alberta, February 27th, 2017

Presentation

- Background: Deterministic dynamical systems approach.
- Contents: Recent tools from dynamical systems (mainly, invariant manifolds), intertwined with the role of stochasticity.
- Aim: Sharing research interests to boost discussion and eventual collaborations.

Outline

1. Part I. Role of noise in bistable perception switches
   - Quasi-periodic perturbations in bistable perception models
   - Part I: conclusions and future work
2. Part II: Phase response curves in transient states
   - Asymptotic phase and isochrons
   - PRFs: extending PRCs in a neighbourhood of a limit cycle
   - Periodic pulse-train stimuli: PRCs vs PRFs
   - Part II: conclusions and future work

Part I. Role of noise in bistable perception switches

Experimental data: perceptual traces and dominance times

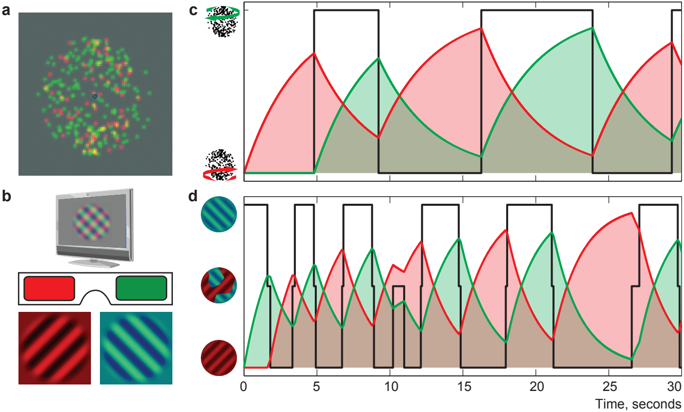

Spontaneous, stochastic events with high variability across stimuli and observers, not completely controlable by intention.

Perceptual traces and dominance times

Dominance times, T_{dom} (black traces), are extracted.

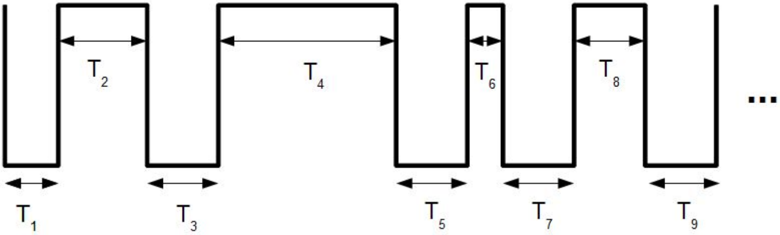

$$< T_{dom} >= \frac{1}{N} \sum_{j=1}^{N} T_j.$$

Stereotypical distribution of dominance times: the Gamma distribution

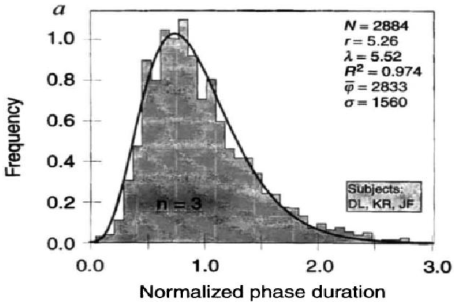

$$f(T) = \lambda^r/\Gamma(r)\exp(-\lambda T)T^{r-1}$$

Logothetis *et. al.*, *Nature*, 380: 621–624, 1996.

Modeling bistable perception

Representative models for bistable perception

Models allowing oscillations

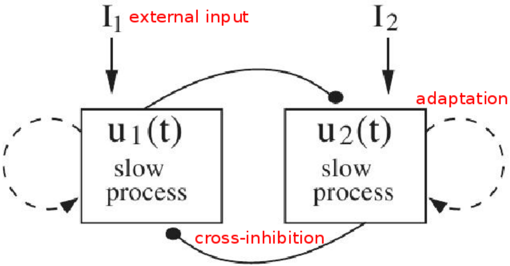

Laing and Chow (2001)

Representative models for bistable perception

Heteroclinic networks

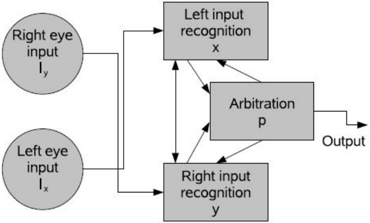

(a)

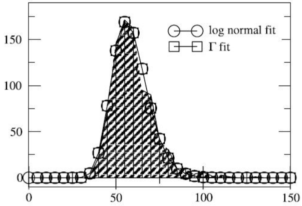

(b)

(a) Model architecture,
(b) Distribution of dominance times

Ashwin and Lavric, *Physica D*, 239: 529–536, 2010.

Representative models for bistable perception

Heteroclinic networks

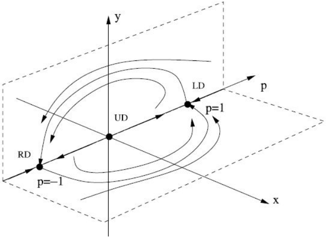

(c)

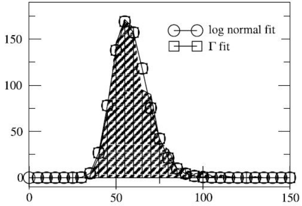

(d)

(c) Schematic phase portrait,
(d) Distribution of dominance times

Ashwin and Lavric, *Physica D*, 239: 529–536, 2010.

The role of noise

Two-attractor models: the Laing-Chow model

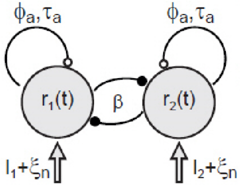

- ***Firing-rate*** variables:

$$\begin{cases} \tau \dot{r}_1 & = -r_1 + f(-\beta r_2 - \phi_a a_1 + I_1 + n_1(t)), \\ \tau \dot{r}_2 & = -r_2 + f(-\beta r_1 - \phi_a a_2 + I_2 + n_2(t)), \end{cases}$$

$\tau \sim 10$ **ms**;

  - β = cross-inhibition;
  - $\phi_{\mathbf{a}}$ = adaptation strength;
  - $\mathbf{I_{1,2}}$ = external stimuli.
  - $f(x) = 1/(1 + exp(-(x - \theta)/k))$ gain function.

Two-attractor models: the Laing-Chow model

- ***Firing-rate*** variables:

$$\begin{cases} \tau \dot{r}_1 & = -r_1 + f(-\beta r_2 - \phi_a a_1 + I_1 + n_1(t)), \\ \tau \dot{r}_2 & = -r_2 + f(-\beta r_1 - \phi_a a_2 + I_2 + n_2(t)), \end{cases} \quad \tau \sim \mathbf{10}\text{ ms};$$

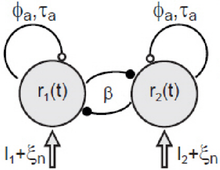

- **Adaptation** variables: $\tau_a \dot{a}_j = -a_j + r_j, \quad j = 1, 2,$ $\tau_a \approx$ 200 **ms**.
- **Noise** dynamics: $d\, n_j = -\frac{n_j}{\tau_n} dt + \sigma_n \sqrt{\frac{2}{\tau_n}} dW_{t,j}, \quad j = 1, 2,$

$\overline{\xi_i(t)\xi_i(t')} = 0$, $\overline{\xi_i(t)} = 0$, $\overline{\xi_i^2(t)} = 1$, $\tau_n \approx$ 100 **ms**.

Bifurcation diagram in the $\phi - \beta$ plane

Basic parameter set: $I_1 = I_2 = 0.5$, $\tau_a = 200$, $k = 0.1$, $\theta = 0.0$.

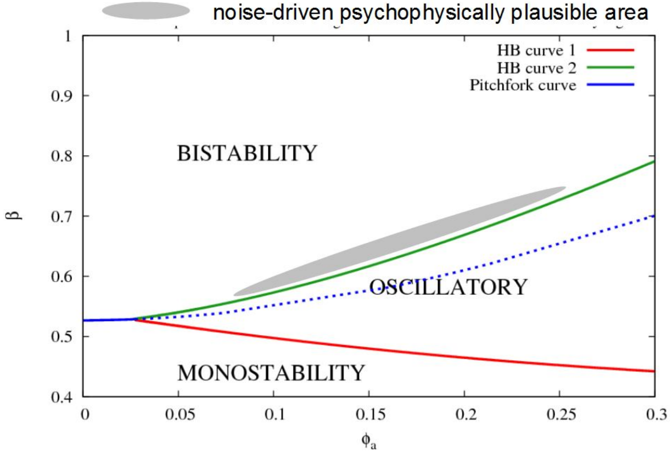

[Moreno-Bote *et. al.*, *J. Neurophysiol.*, 2007], [Pastukhov *et. al.*, *Frontiers Comp. Neur.*, 2013], from experimental data that matches the grey spot for several models.

The effect on the time distributions

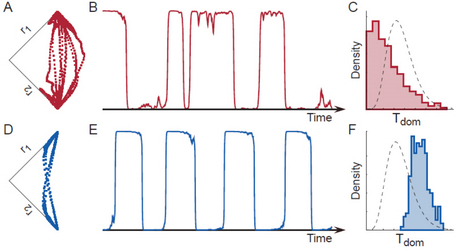

(A-B-C) Driven largely by noise: irregular trajectories (A), aperiodic dominance reversals (B), and approx. exponential distribution of T_{dom} (C).
(D-E-F) Driven largely by adaptation: regular trajectories (D), periodic dominance reversals (E), and approx. Gaussian distribution of dominance times (F).

The multi-stable dynamics of **human observers** falls between these two extremes, exhibiting a **Gamma-like distribution** of T_{dom} (dashed curves in C and F).

Questions (motivation)

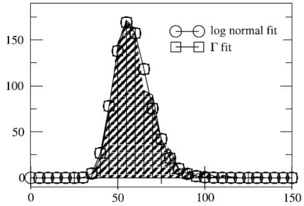

Time distribution in a heteroclinic network with noise [Ashwin-Lavric, Phys D 2010]

- What is this **noise** modeling: noise in the stimulus, high variability in input sources, internal noise,. . . ?
- What is the **level of complexity** of the inputs to achieve this time-dominance distributions? Or, we must assume that perceptual events are influenced by inputs filling in a **continuum of frequencies** as noise implies?

Quasi-periodic perturbations in bistable perception models

Heteroclinic models: winnerless competition

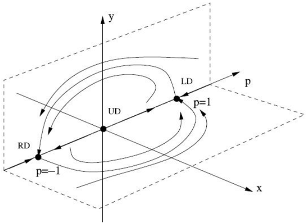

- p: arbitration (underlying activity); $p = 1$ means LD (left dominant; $p = -1 \Leftrightarrow$ RD.
- x: activity pattern associated w/ stimulus to the **left** eye.
- y: activity pattern associated w/ stimulus to the **right** eye.

- Winnerless competition is replaced by an **approximately periodic switching** between both states: $p = 1$ (LD) and $p = -1$ (RD).
- Fixed points $(\pm 1, 0, 0)$ are **saddles**. No need of adaptation variables: *slow* flow provided by passage nearby saddles.

Ashwin and Lavric, *Physica D*, 239: 529–536, 2010.

Heteroclinic models: winnerless competition

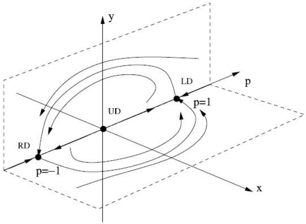

$$\begin{cases} \dot{p} &= h(p) + x^2(1-p) + y^2(-1-p) + \eta_p(t), \\ \dot{x} &= f(p,x,y) + I_x\, x + \eta_x(t), \\ \dot{y} &= f(-p,y,x) + I_y\, y + \eta_y(t), \end{cases}$$

- $h(p) = -p(p-1)(p+1)$;
  $f(p,x,y) = \left((0.5-p)(p+1) - x^2 - y^2\right)\, x$.
- $I_{\{x,y\}}$: external inputs.
- $\eta_{\{x,y\}}$: biased Wiener noise (mean $\mu_{\{x,y\}}$ and variance per unit time $\sigma_{\{x,y\}}$). [Ashwin and Lavric, Physica D (2010)]

Heteroclinic model: quasi-periodic forcing

$$\begin{cases} \dot{p} &= h(p) + x^2(1-p) + y^2(-1-p), \\ \dot{x} &= f(p,x,y) + I_x\, x + \epsilon \sum_{i=0}^{M} n_{x\,i} \cos(\theta_i), \\ \dot{y} &= f(-p,y,x) + I_y\, y + \epsilon \sum_{i=0}^{M} n_{y\,i} \cos(\theta_i), \\ \dot{\theta}_j &= \omega_j, \quad j = 1,\ldots,M,\ \theta \in \mathbb{T}^M. \end{cases}$$

- Defining $F := p^2 + 2\,x^2 - 1$ and $G := p^2 + 2\,y^2 - 1$, the **heteroclinic connections** are given by $S_\mp := \{F = 0\} \cap \{y = 0\}$ and $S_\pm := \{G = 0\} \cap \{x = 0\}$ (figure from [Ashwin and Lavric, *PhysD* (2010)]).

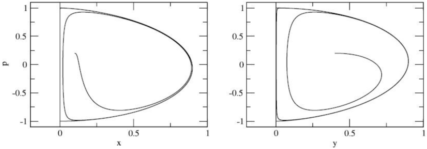

$S_\mp$ and $S_\pm$, respectively.

Separatrix map (SM) for the heteroclinic network

Poincaré sections

Global view

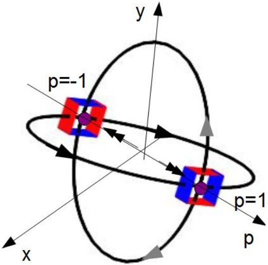

Partial view

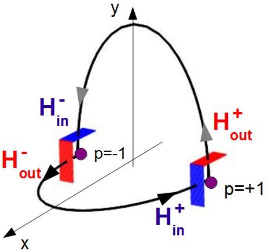

Local view

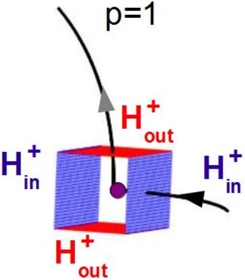

SM for the heteroclinic network: map components

$L^+ : (F_0, y_0, \theta_0) \mapsto (G_1, x_1, \theta_1)$

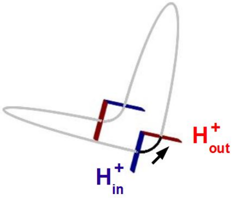

$T_G^{\mp} : (F_3, y_3, \theta_3) \mapsto (F_0, y_0, \theta_0)$

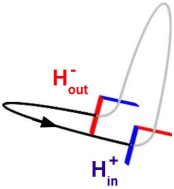

$T_G^{\pm} : (G_1, x_1, \theta_1) \mapsto (G_2, x_2, \theta_2)$

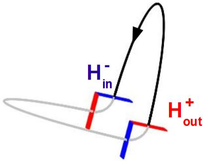

$L^- : (G_2, x_2, \theta_2) \mapsto (F_3, y_3, \theta_3)$

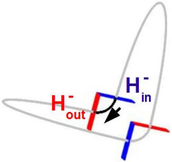

Total Poincaré map

Linearizing the flow close to the saddles and applying Melnikov theory for the global maps:

$$\Pi := T_G^{\mp} \circ L^- \circ T_G^{\pm} \circ L^+ : H_{in}^+ \longrightarrow H_{in}^+$$

$\mathbf{L^+} : \mathbf{H_{in}^+} \longrightarrow \mathbf{H_{out}^+}$

$$\begin{aligned}
x_1 &= r_x \left(\frac{r_y}{y_0}\right)^{-(1-l_x)/l_y}, \\
G_1 &= F_0\psi^2 - 2\, r_x(\psi^2 - 1) \\
&= +2\left(-1 + \sqrt{1 + F_0 - 2\, r_x^2}\right)\psi(1-\psi), \\
\theta_1 &= \theta_0 + \omega \frac{1}{l_y} \ln \frac{r_y}{y_0}. \\
\psi &:= \left(\frac{r_y}{y_0}\right)^{-2/l_y}
\end{aligned}$$

$\mathbf{T_G^{\pm}} : \mathbf{H_{out}^+} \longrightarrow \mathbf{H_{in}^-}$

$$\begin{aligned}
x_2 &= \hat{\alpha}\, x_1 + \hat{f}(\theta; l_x, \epsilon), \\
G_2 &= \alpha\, G_1 + f(\theta; l_x, \epsilon), \\
\theta_2 &= \theta_1 + \omega\,(T_2 - T_1).
\end{aligned}$$

$\mathbf{T_G^{\mp}} : \mathbf{H_{out}^-} \longrightarrow \mathbf{H_{in}^+}$

(similar to $T_G^{\pm}$)

$\mathbf{L^-} : \mathbf{H_{in}^-} \longrightarrow \mathbf{H_{out}^-}$

(similar to L^+)

Numerical example

Time dominance distributions for the HN with 1,2,3 frequencies and noise; $r = 0.1$, $\varepsilon = 0.001$ and $I_x = I_y = 0.01$; $\omega_1 = 1$, $\omega_2 = \frac{\sqrt{5}-1}{2}$ and $\Omega \approx 0.6823$.

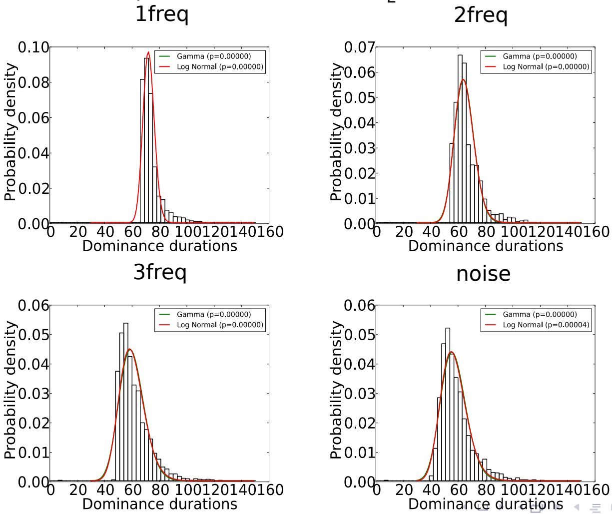

Part I: conclusions and future work

- **Main question:** What is the **minimal degree of complexity** to explain switches in bistable perception psycophysical experiments?
- We obtain Gamma distributions of time dominance series with quasi-periodic stimuli (with 2 non-resonant frequencies or more).
- We give analytical support to the models by using the separatrix map.
- We provide maps that can be considered as alternative (discrete) models for bistable perception, which avoid numerical unstability when integrating close to saddle points.
- **Future work:** how to use it for fitting experimental (psychophysical) data?

Part II: Phase response curves in transient states

Response to a stimulus

- We want to know the sensitivity of an oscillator (limit cycle) to a stimulus received at different phases of the oscillation.
- Important to study entrainment and synchronization, see for instance [R.F. Galán, G.B. Ermentrout, N.N. Urban (2005-2008)], [S.A. Oprisan, C. Canavier *et al,* (2002-. . .)],. . .

Phase variation, phase response curves (PRCs)

“Heuristic" computation of the phase variation:

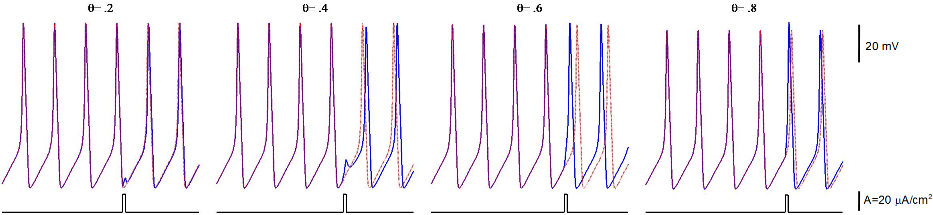

Phase variation, phase response curves (PRCs)

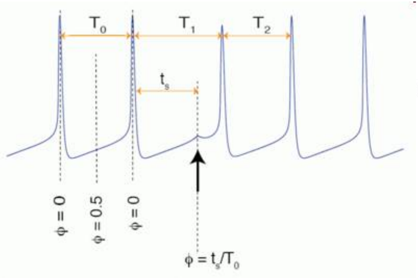

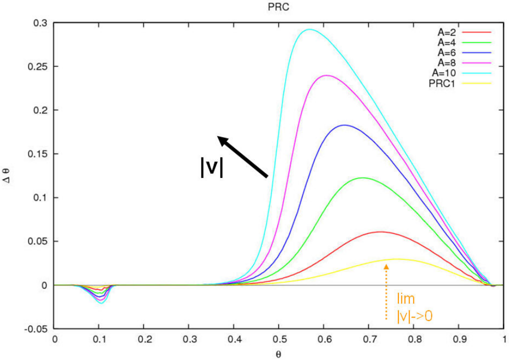

The phase advancement/delay due to an external input at time t_s is given by

$$\Delta\theta = \frac{T - T_1(t_s, v)}{T}, \ \theta = t_s/T.$$

$T = T_0$ in the left figure

Infinitesimal PRC (**weak** brief pulse): the “classical" theory

Consider a system instantaneously perturbed by a small perturbation in a direction $\mathbf{v} \in \mathbb{R}^d$:

$$\dot{x} = X(x) + \varepsilon \mathbf{v}\, \delta(t - t_s).$$

If $x(t)$ is the solution of the unperturbed system, the solution of the perturbed one at time t_s is $x(t_s) + \varepsilon \mathbf{v}$.

To compute the difference between their phases we can use Taylor:

$$\Theta(x(t_s) + \varepsilon \mathbf{v}) - \Theta(x(t_s)) = \varepsilon \nabla\Theta(x(t_s)) \cdot \mathbf{v} + O(\varepsilon^2).$$

One defines the **infinitesimal PRC** as: $iPRC(\Theta(x), \mathbf{v}) = \nabla\Theta(x) \cdot \mathbf{v}$

The Adjoint method

[Malkin 1949-1956, Ermentrout and Kopell 1991, Hoppensteadt and Izhikevich 1997, Ermentrout 2002]

$\nabla\Theta$ along the limit cycle (the PRC) is given by the T-periodic solution of the **adjoint equation**

$$\frac{dQ}{dt} = -DX^T(\gamma(t))Q, \tag{1}$$

satisfying the condition

$$Q(\gamma(t)) \cdot X(\gamma(t)) = \frac{1}{T}$$

- The adjoint equation allows one to compute $\nabla\Theta$ on the limit cycle without knowing Θ beyond.
- The neuron must be on the asymptotic state, so brief, weak stimuli and fast convergence are required.
- But . . .

PRFs: extending the PRCs...

Motivation.

...neither all stimuli are brief, weak enough nor the attractors are strong enough:

- Repeated stimulations far from the limit cycle: short stimulation periods, bursting-like stimuli, random fluctuations,...
- Low characteristic exponents.
- Large stimulus amplitude.

For these purposes, there is a need for more *precise* knowledge of isochrons and PRCs beyond the limit cycle itself.

Main purpose

1. Provide tools (via the computation of isochrons) useful for more general instances than weak coupling or brief stimuli.
2. Analyze effects of a perturbation in the transient states; that is, when the dynamics has not relaxed back to the limit cycle. Due to factors like: short stimulation periods, slow attraction to the limit cycle or low characteristic multipliers, large stimulus amplitude, random fluctuations, bursting-like stimuli, . . .

[A. G., G. Huguet, SIADS (2009)]

[O. Castejón, A. G., G. Huguet, J. Math. Neuro. (2013)]

[O. Castejón, A. G., preprint (2017]

The mathematical framework

Consider an autonomous system of ODEs

$$\dot{x} = X(x), \quad x \in \mathbb{R}^d, d \geq 2$$

with a periodic orbit γ of period T parameterized by the phase $\theta = t/T$.

A point $q \in \Omega \subset \mathbb{R}^d$, $\gamma \subset \Omega$, is in asymptotic phase with a point $p \in \gamma$ if

$$\lim_{t \to \infty} |\Phi_t(q) - \Phi_t(p)| = 0,$$

with $\Phi_t(x)$ the trajectory of X s.t. $\Phi_0(x) = x$.

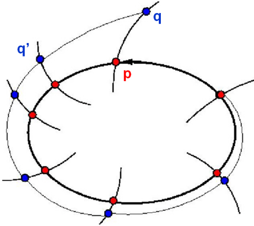

The set of points having the same asymptotic phase is called isochron. The asymptotic phase is $\Theta : \Omega \subset \mathbb{R}^d \to \mathbb{T} = [0, 1)$, such that $\Theta(\gamma(\theta)) = \theta$, and $\Theta(p) = \Theta(q)$ if p and q lie on the same isochron. See also [J.T.C. Schwabedal, A. Pikovsky (2010, 2013)], [P. Thomas, B. Lindner (2015)] for a stochastic version.

Isochrons: graphical representations

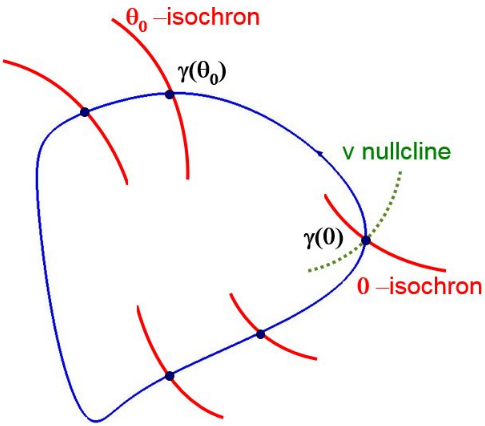

Application of the parameterization method

- Isochrons can be seen as the stable manifolds of the points of the limit cycle.
- We look for a map K such that

$$\left(\frac{1}{T}\partial_\theta + \frac{\lambda\sigma}{T}\partial_\sigma\right) K(\theta,\sigma) = X(K(\theta,\sigma)), \tag{2}$$

  where λ is the characteristic exponent of γ, see [Cabré, Fontich, de la Llave, 2005].
- Motion generated by X expressed in (θ,σ):

$$\begin{aligned} \dot\theta &= 1/T, \\ \dot\sigma &= \lambda\sigma/T. \end{aligned}$$

- One has $\Theta(K(\theta,\sigma)) = \theta$, so that $K(\theta^*,\sigma)$ is the θ^*-isochron.

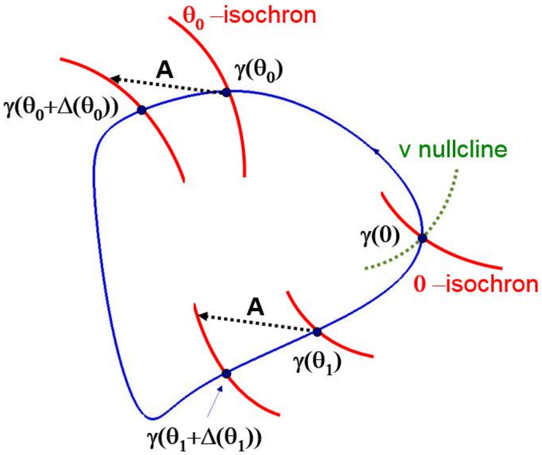

$$\theta_1 - \theta_0 \approx \varepsilon \nabla \Theta \cdot v$$

$$\sigma_1 - \sigma_0 \approx ??$$

The adjoint method extended

[G-Huguet, 2009]

- Recall, the phase variation is given by:

$$\Theta(p+\varepsilon\mathbf{v}) - \Theta(p) = \varepsilon\nabla\Theta(p)\cdot\mathbf{v} + O(\varepsilon^2).$$

  Now $p \in \Omega$. That is, it might not be on the limit cycle.

- The Phase Resetting Function (PRF) for any $p \in \Omega$, $p = K(\theta,\sigma)$, is given by

$$\nabla\Theta(p) = \frac{\partial_\sigma K^\perp(\theta,\sigma)}{T < \partial_\sigma K^\perp(\theta,\sigma), X(K(\theta,\sigma)) >}$$

- One has that $\nabla\Theta$ along the orbits of the vector field X, satisfies the same adjoint equation (1):

$$\frac{dQ}{dt} = -DX^T(\phi_t(p))Q,$$

where ϕ_t is the flow of X, with the initial condition

$$Q(0) = \frac{\partial_\sigma K^\perp(\theta,\sigma)}{T < \partial_\sigma K^\perp(\theta,\sigma), X(K(\theta,\sigma)) >}.$$

- One can find $K(\theta,\sigma)$ numerically and thus obtain $\nabla\Theta$.

Amplitude Resetting Functions

[Castejón-G-Huguet, 2013]

- We can consider the first order of the variation of the variable σ after a brief stimulus
- One can define a function $\Sigma : \Omega \to \mathbb{R}$ such that $\Sigma(K(\theta, \sigma)) = \sigma$. Then one has:

$$\Sigma(p + \varepsilon \mathbf{v}) - \Sigma(p) = \varepsilon \nabla\Sigma(p) \cdot \mathbf{v} + O(\varepsilon^2)$$

- We call $\nabla\Sigma \cdot \mathbf{v}$ the Amplitude Resetting Function (ARF)

- Similarly as we did for the $\nabla\Theta$, we have for $p = K(\theta, \sigma)$:

$$\nabla\Sigma(p) = \frac{\lambda\sigma\, \partial_\theta K^{\perp}(\theta, \sigma)}{T < \partial_\theta K^{\perp}(\theta, \sigma), X(K(\theta, \sigma)) >}$$

.

- $\nabla\Sigma$ along the orbits of X satisfies a kind of adjoint equation:

$$\frac{dQ}{dt} = \left(\frac{\lambda}{T} Id - DX^T(\phi_t(p)) \right) Q$$

.

- One can find also $\nabla\Sigma$ numerically.

Summarizing...

- "Classical version": PRC on $\gamma \cong \mathbb{S}^1$.
- "Extended version": PRFs and ARFs on $\Omega \cong \mathbb{S}^1 \times (\sigma_{low}, \sigma_{up})$, with $0 \in (\sigma_{low}, \sigma_{up})$.

In the following, we take $\mathbf{v} = (1, 0)$ and denote $\nabla\Theta(x) \cdot \mathbf{v}$ by PRF(x) and $\nabla\Sigma(x) \cdot \mathbf{v}$ by ARF(x).

Periodic pulse-train stimuli: PRCs vs PRFs

We stimulate periodically the system with pulses, with period $T_s < T_0$. We consider both:

1D approach $$\theta_j = \theta_{j-1} + \varepsilon PRC(\theta_{j-1}) + T_s/T_0, \quad (\text{mod } 1)$$

2D-approach $$\begin{cases} \theta_j &= \theta_{j-1} + \varepsilon PRF(\theta_{j-1}, \sigma_{j-1}) + T_s/T_0, \quad (\text{mod } 1) \\ \sigma_j &= (\sigma_{j-1} + \varepsilon ARF(\theta_{j-1}, \sigma_{j-1})) \exp(\lambda\, T_s/T_0), \end{cases}$$

This allows to compare Poincaré maps for 1D PRCs with those for 2D PRFs-ARFs. Some examples have shown differences: phase locking at different phase, phase locking vs periodic orbits in phase,...

A toy model

Consider the system in polar coordinates,

$$\begin{cases} \dot{r} &= \alpha\, r(1 - r^2), \\ \dot{\phi} &= 1 + \alpha\, a\, r^2, \end{cases}$$

having a limit cycle γ of period $T = 2\pi/(1 + \alpha\, a)$, parameterized by $\theta \in [0, 1)$ as $\gamma(\theta) = (\cos(2\pi\theta), \sin(2\pi\theta))$.

- We can compute explicitly $K(\theta, \sigma)$, $PRF(\theta, \sigma)$ and $ARF(\theta, \sigma)$
- α determines the rate of attraction of the limit cycle
- a determines the relative position of the isochrons to the limit cycle
- We compute the exact change of phase, and the 1D and 2D approaches. Compare them using rotation numbers

A toy model

Consider the system in polar coordinates,

$$\begin{cases} \dot{r} &= \alpha\, r(1 - r^2), \\ \dot{\phi} &= 1 + \alpha\, a\, r^2, \end{cases}$$

having a limit cycle γ of period $T = 2\pi/(1 + \alpha\, a)$, parameterized by $\theta \in [0, 1)$ as $\gamma(\theta) = (\cos(2\pi\theta), \sin(2\pi\theta))$.

- We can compute explicitly $K(\theta, \sigma)$, $PRF(\theta, \sigma)$ and $ARF(\theta, \sigma)$
- α determines the rate of attraction of the limit cycle
- a determines the relative position of the isochrons to the limit cycle
- We compute the exact change of phase, and the 1D and 2D approaches. Compare them using rotation numbers

Parameterization and response functions for the toy model

$$K(\theta, \sigma) = \left(\sqrt{\frac{1}{1 - 2\alpha\sigma}} \cos(\Omega), \sqrt{\frac{1}{1 - 2\alpha\sigma}} \sin(\Omega) \right),$$

$$PRF(K(\theta, \sigma)) = -\frac{\sqrt{1 - 2\alpha\sigma}}{2\pi} (\sin(\Omega) - a\cos(\Omega)).$$

$$ARF(K(\theta, \sigma)) = \frac{(1 - 2\alpha\sigma)^{3/2}}{\alpha} \cos(\Omega),$$

where $\Omega := 2\pi\theta + \frac{1}{2} a \ln(1 - 2\alpha\sigma)$.

First exploration: Simulations

- 1D map: θ_j and plot $K(\theta_j, 0)$.
- 2D map: (θ_j, σ_j) and plot $K(\theta_j, \sigma_j)$
- **Exact map**: We define

$$(\tilde{\theta}_j, \tilde{\sigma}_j) = K^{-1}(K(\theta_j, \sigma_j) + \varepsilon \mathbf{v}).$$

Then we plot: $K(\tilde{\theta}_j + T_s/T_0, \tilde{\sigma}_j \exp(\lambda T_s/T_0))$.

What are the similarities or differences among these three maps?

Rotation numbers

$$\rho = \lim_{N\to\infty} \frac{1}{N} \sum_{j=1}^{N} (\theta_j - \theta_0)$$

Comparison between rotation numbers of 1D-map versus the exact map: relative error of the 1D approach, e_1.

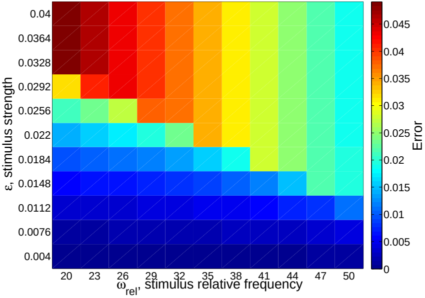

Rotation numbers

$$\rho = \lim_{N\to\infty} \frac{1}{N} \sum_{j=1}^{N} (\theta_j - \theta_0)$$

Comparison between rotation numbers of 2D-map versus the exact map: relative error of the 2D approach, e_2.

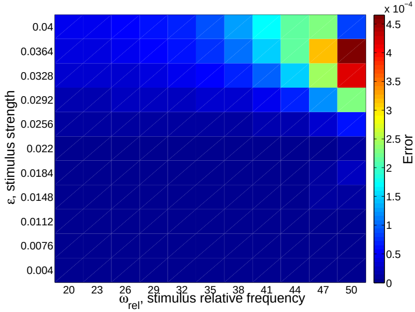

Rotation numbers

$$\rho = \lim_{N \to \infty} \frac{1}{N} \sum_{j=1}^{N} (\theta_j - \theta_0)$$

Comparison between rotation numbers of 1D-map versus 2D-map: e_2/e_1.

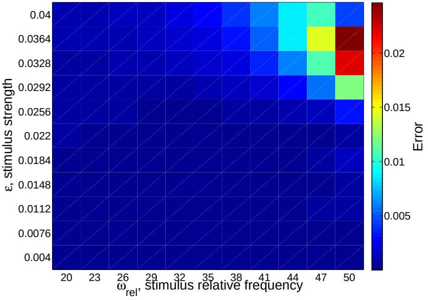

A reduced Hodgkin-Huxley model: isochrons and isostables

We also compute rotation numbers for a reduced Hodgkin-Huxley model (numerics requires much more work):

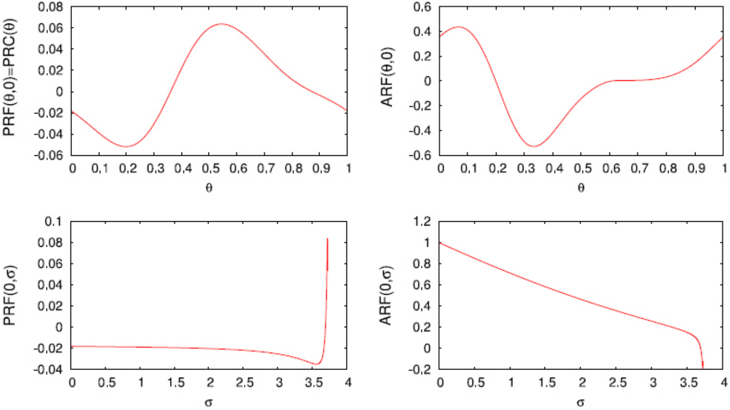

Simulations: increasing ε

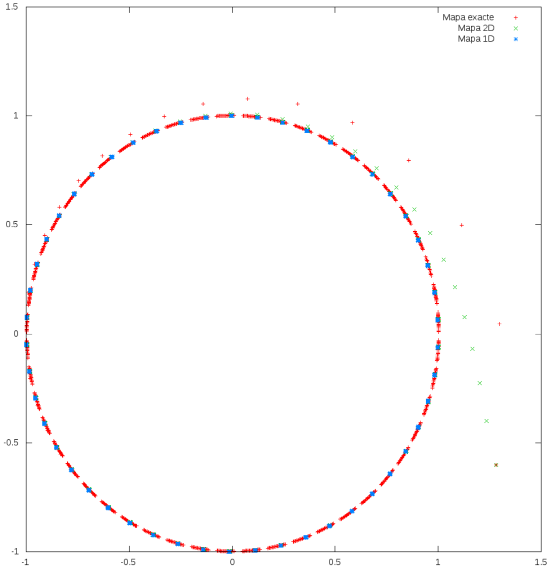

Simulations: increasing ε

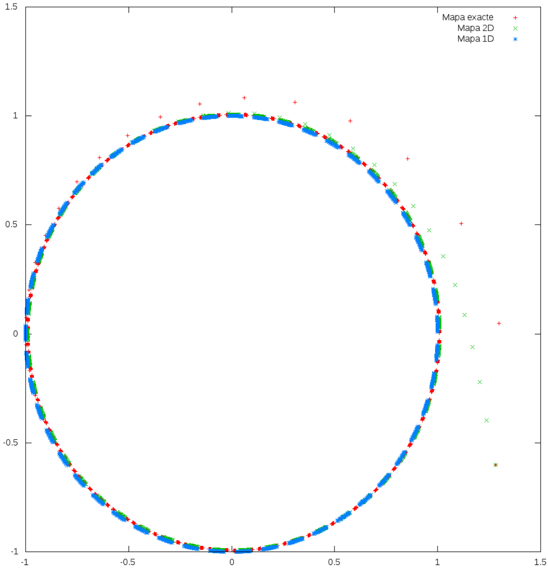

Simulations: increasing ε

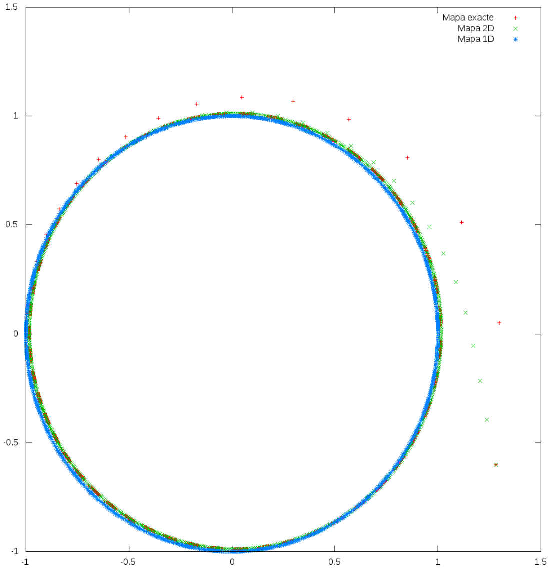

Simulations: increasing ε

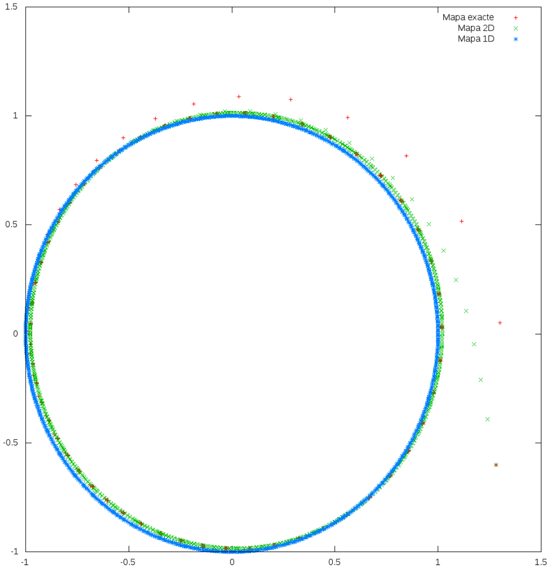

Simulations: increasing ε

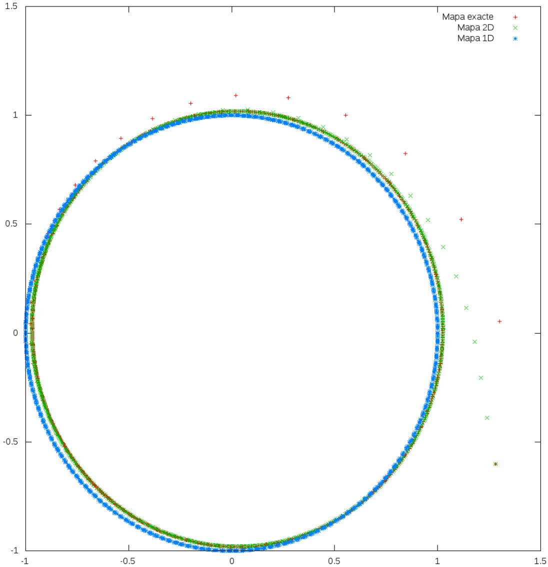

Simulations: increasing ε

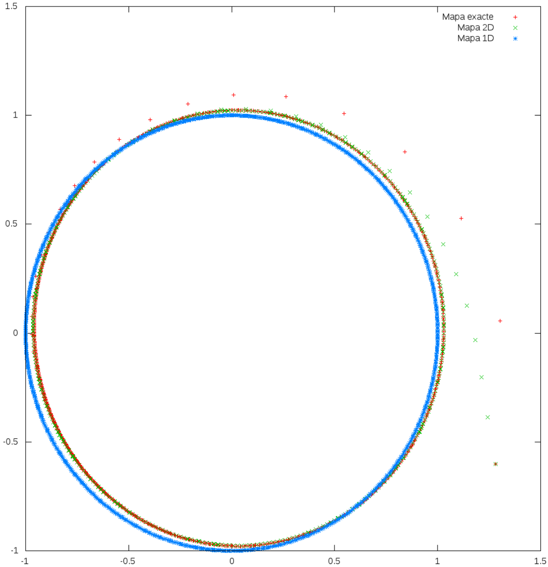

Simulations: increasing ε

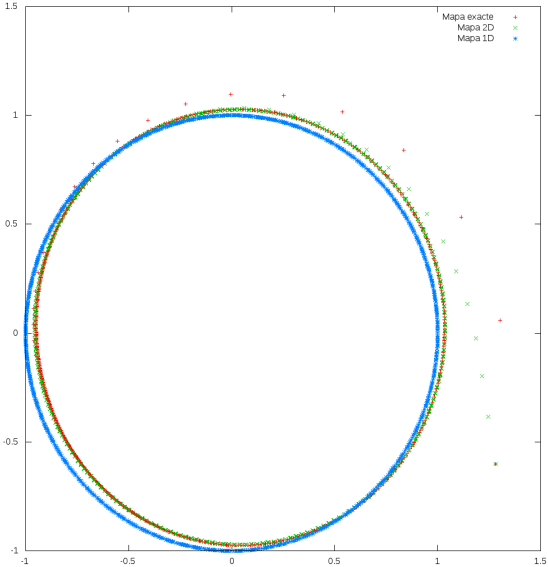

Simulations: increasing ε

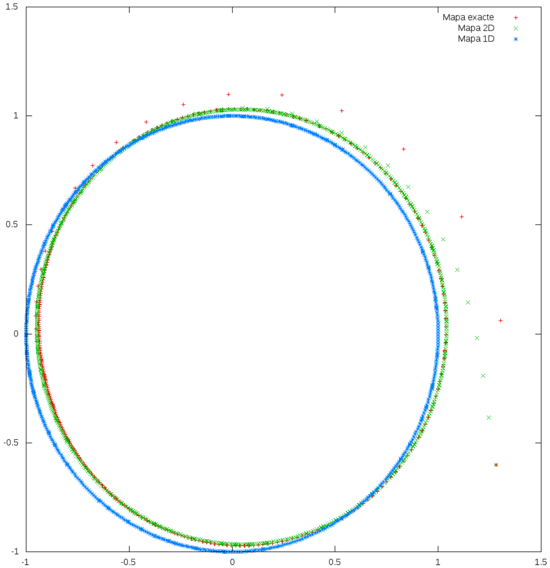

Simulations: increasing ε

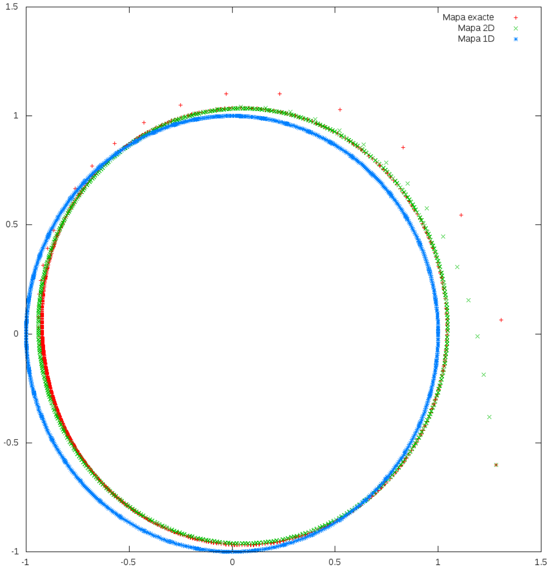

Simulations: increasing ε

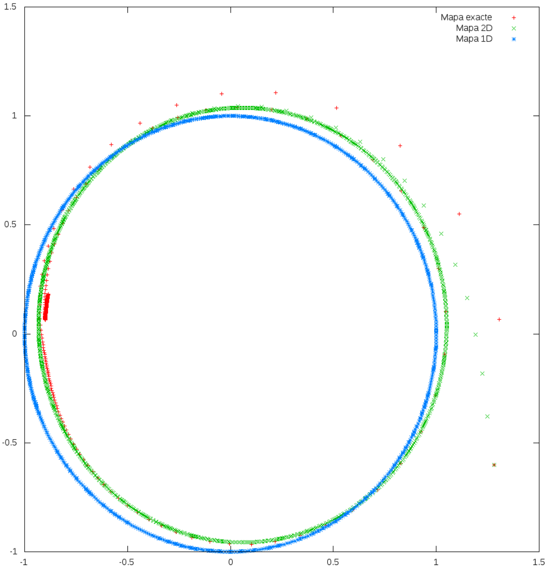

Simulations: increasing ε

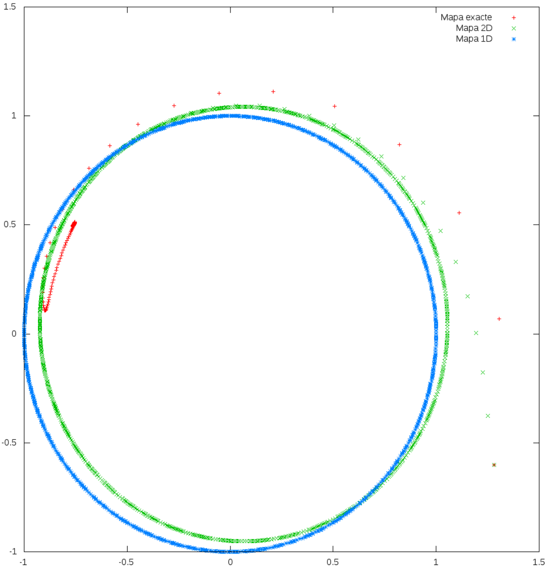

Simulations: increasing ε

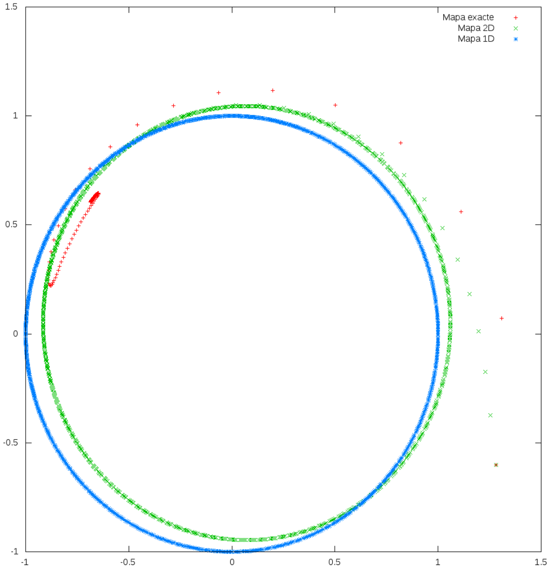

Simulations: increasing ε

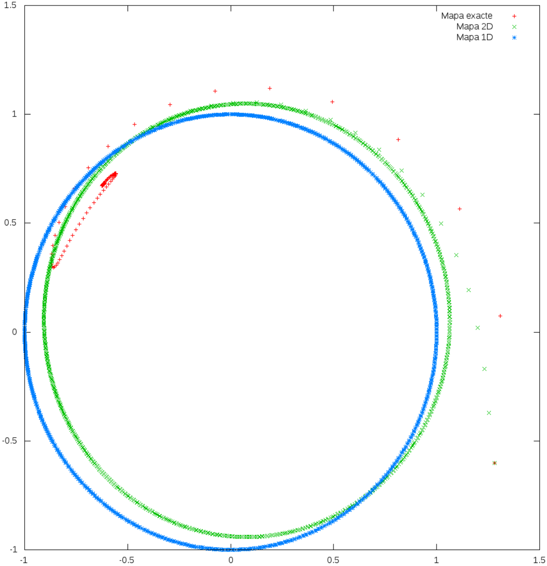

Simulations: increasing ε

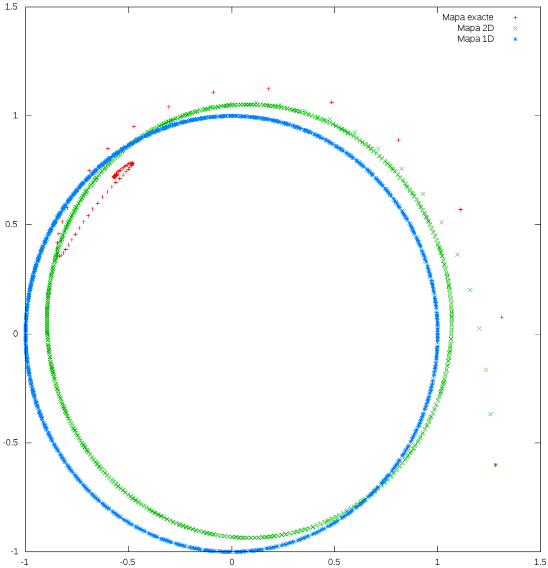

Simulations: increasing ε

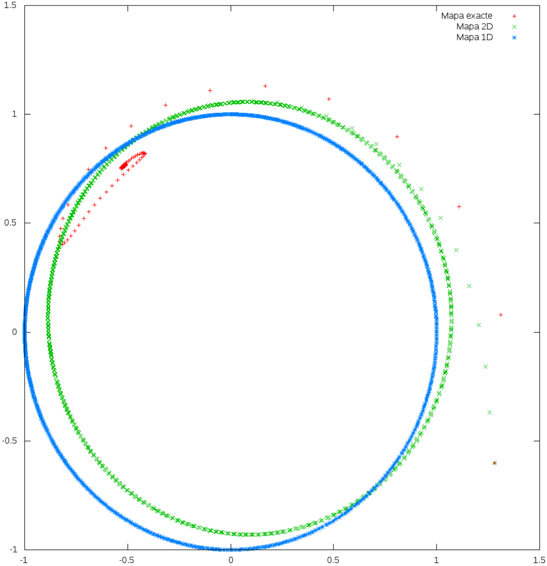

Simulations: increasing ε

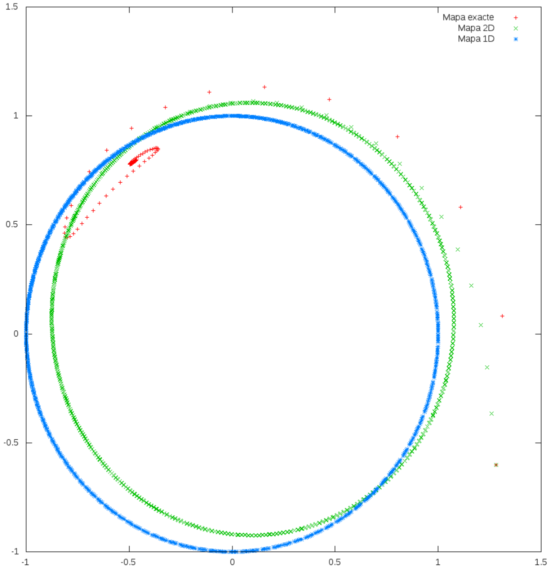

Simulations: increasing ε

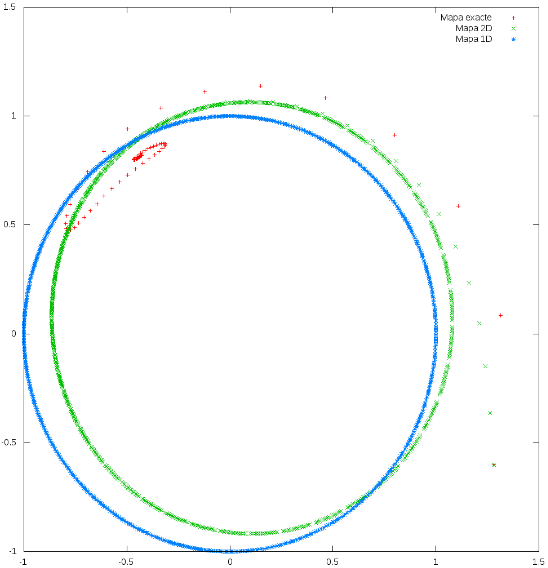

Simulations: increasing ε

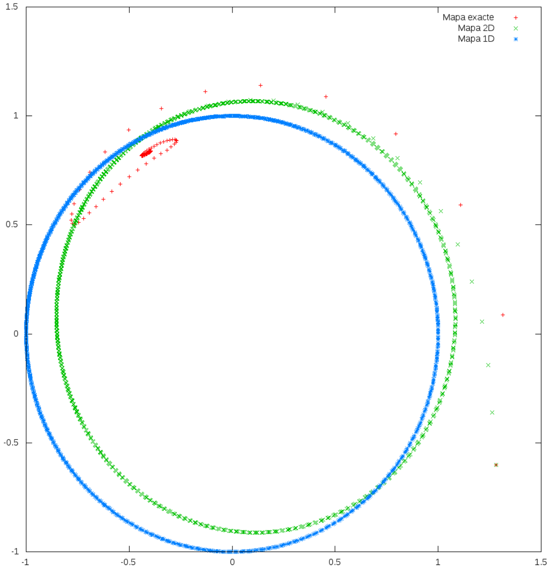

Simulations: increasing ε

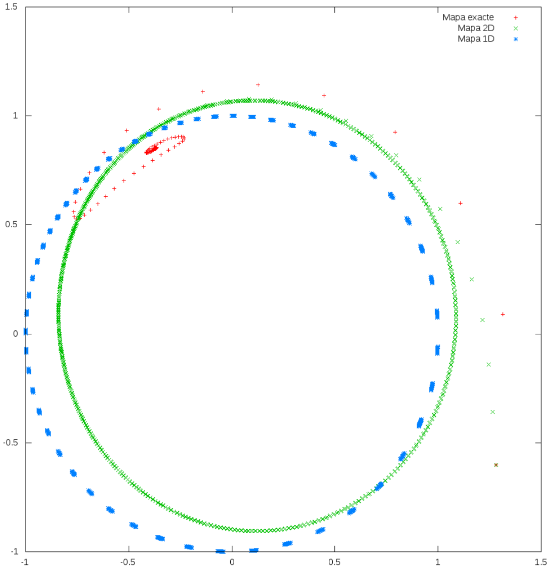

Simulations: increasing ε

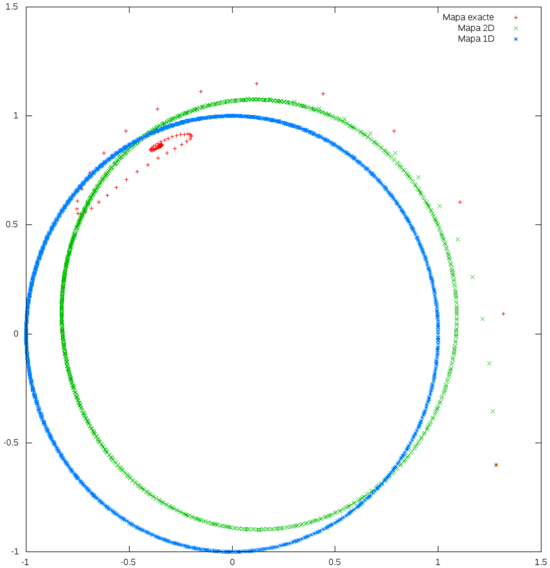

Simulations: increasing ε

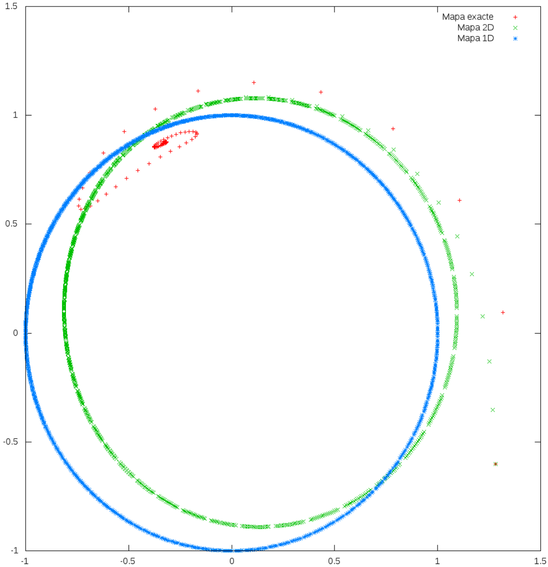

Simulations: increasing ε

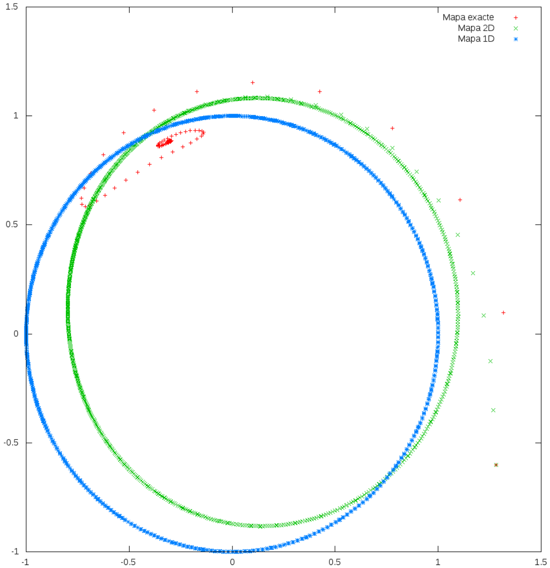

Simulations: increasing ε

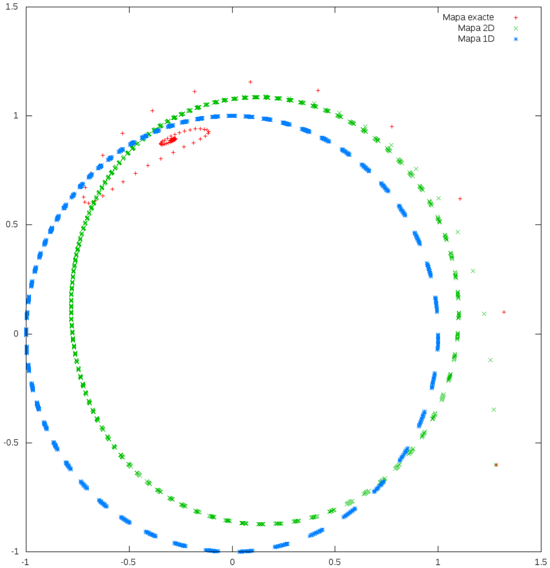

Simulations: increasing ε

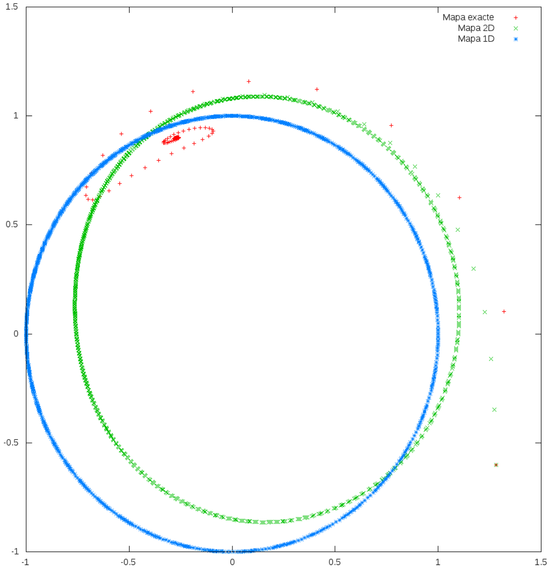

Simulations: increasing ε

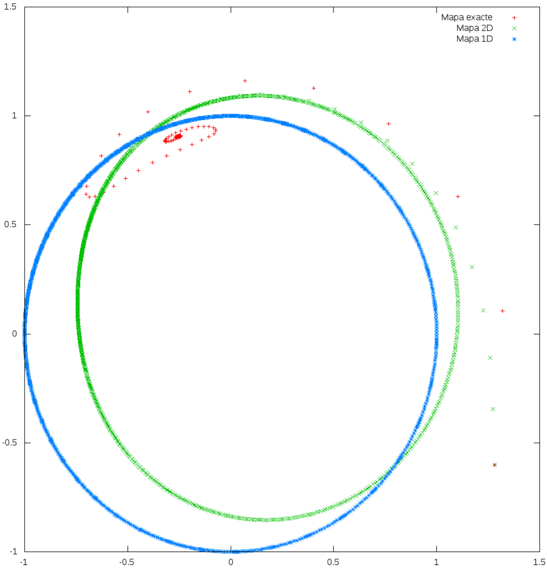

Simulations: increasing ε

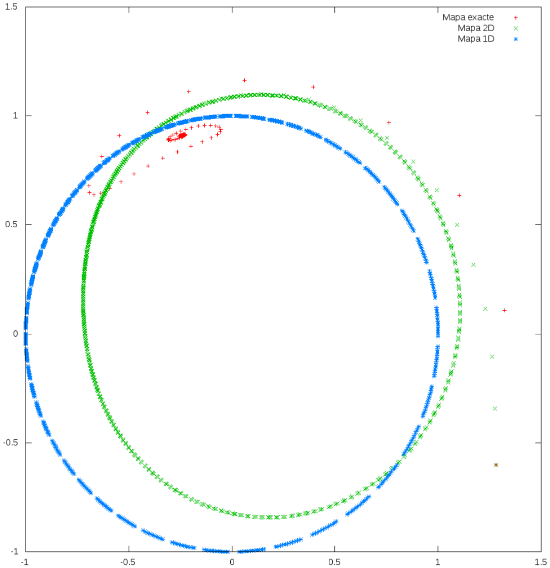

Simulations: increasing ε

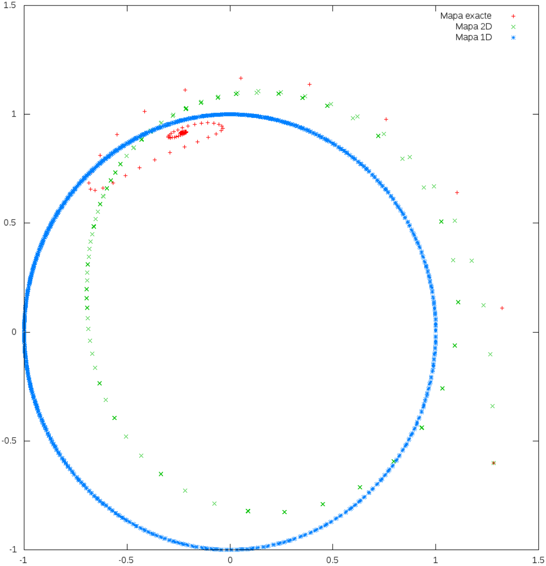

Simulations: increasing ε

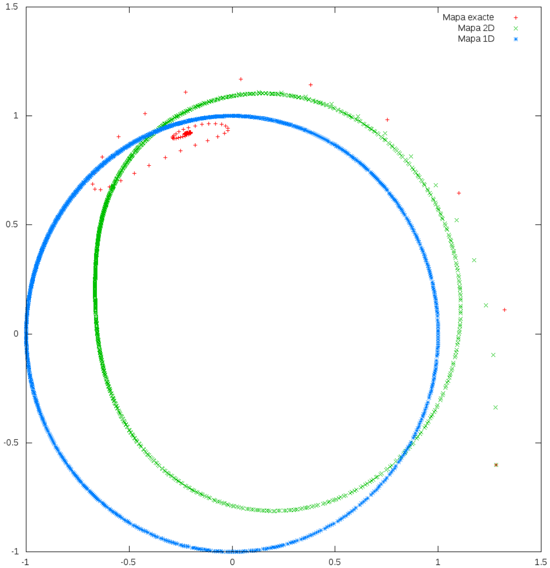

Simulations: increasing ε

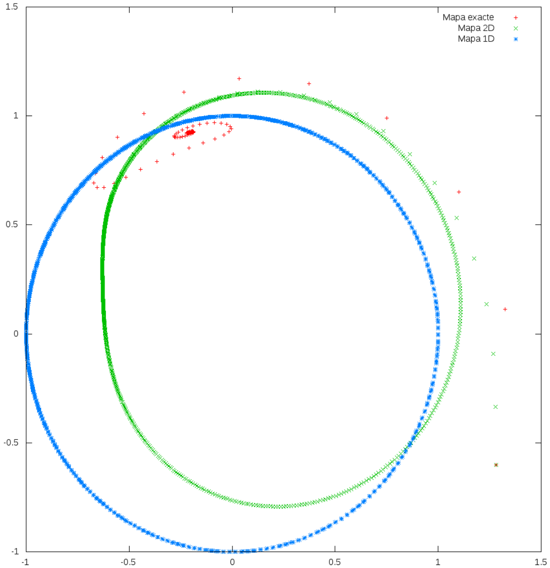

Simulations: increasing ε

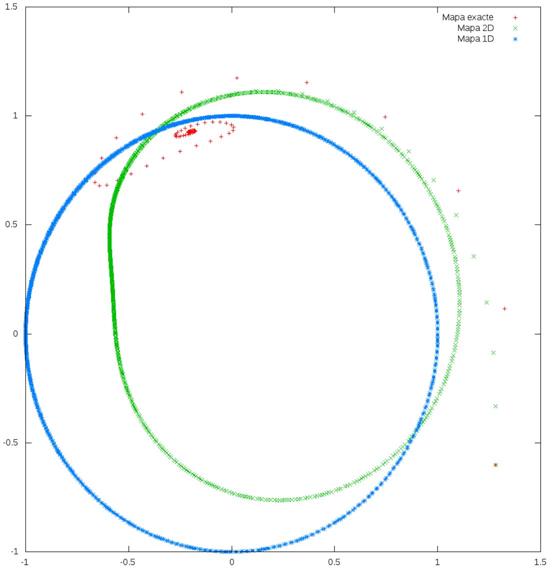

Simulations: increasing ε

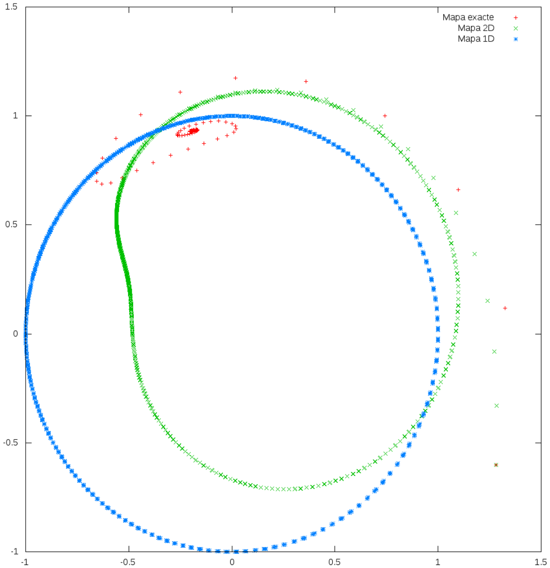

Simulations: increasing ε

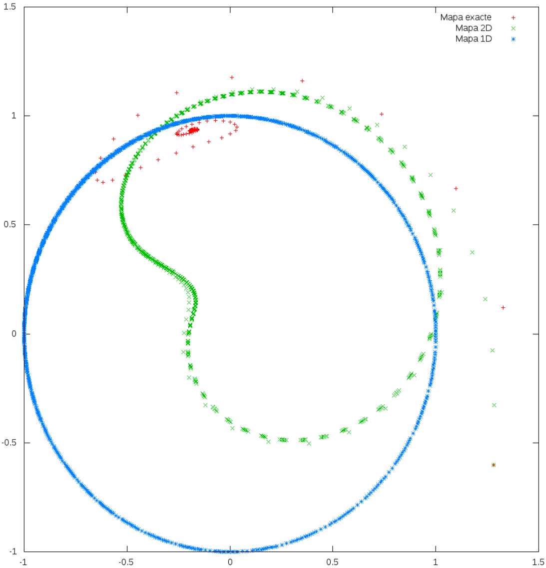

Simulations: increasing ε

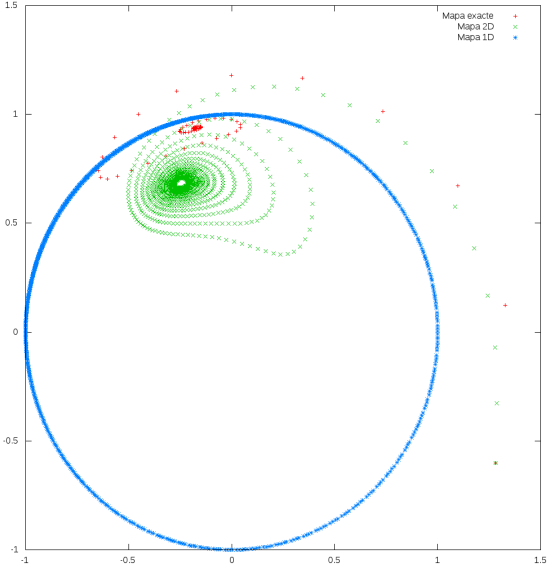

Simulations: increasing ε

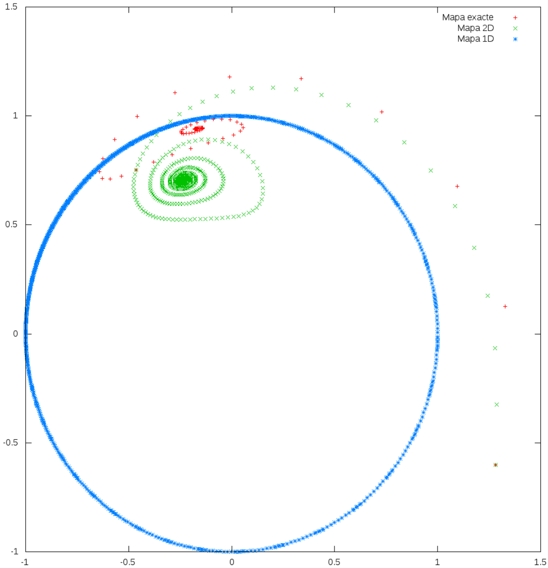

Simulations: increasing ε

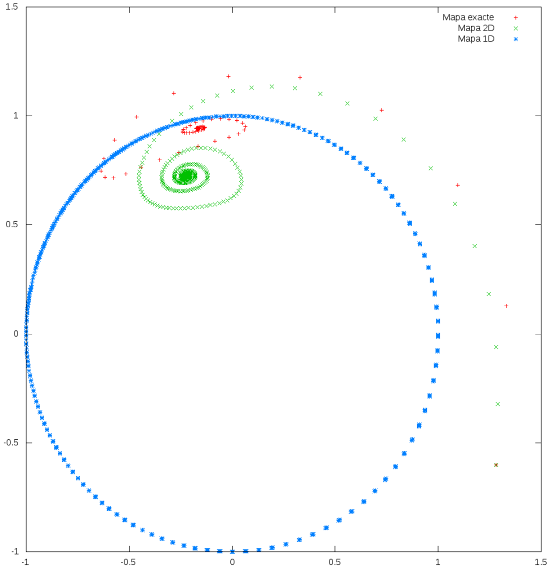

Simulations: increasing ε

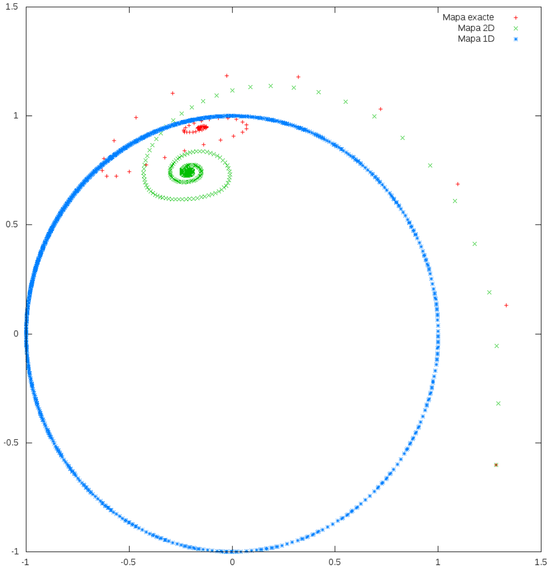

Simulations: increasing ε

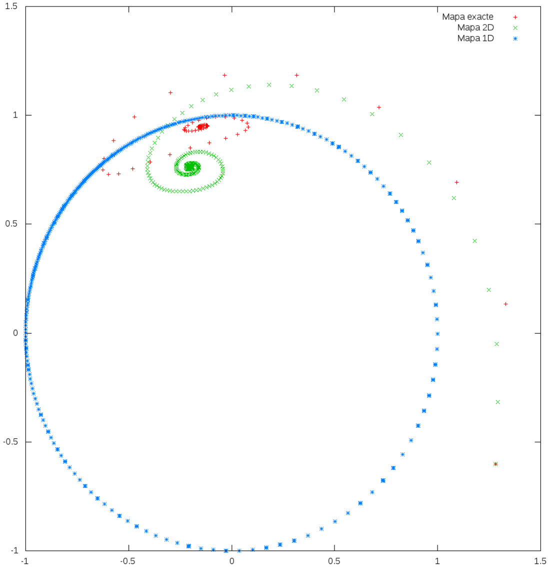

Simulations: increasing ε

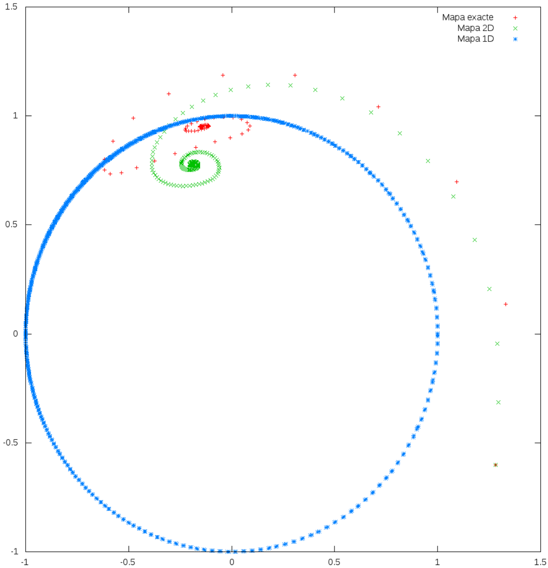

Simulations: increasing ε

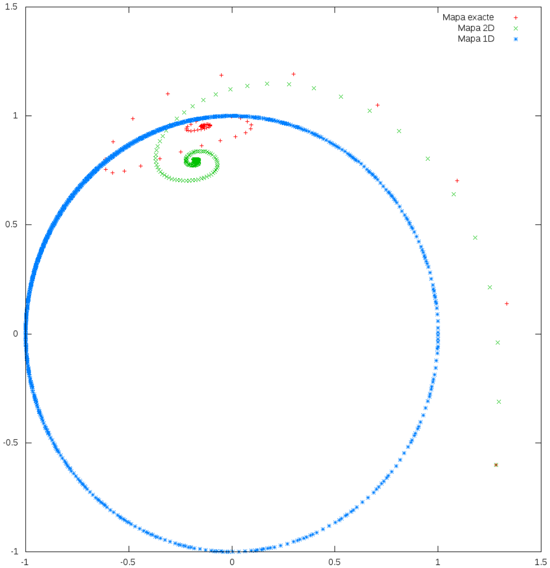

Simulations: increasing ε

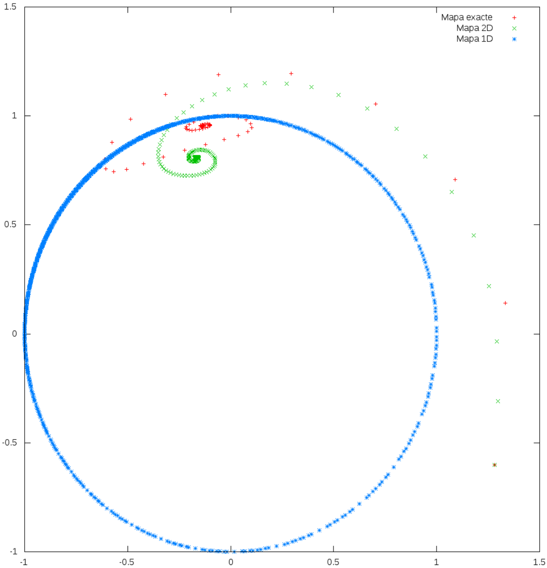

Simulations: increasing ε

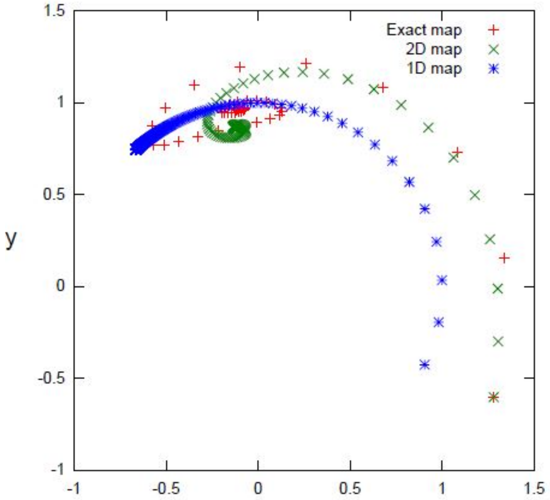

Conclusions, remarks and future work I

- We extend the notion of PRC to the generalized response functions PRF-ARF, which allows to have a more accurate prediction of the response of a neuron to an external stimulus. It becomes relevant when this stimulus is not weak or has a high frequency (neuronal dynamics spends more time on the transient state rather than the asymptotic state).
- In dimensions higher than 2, it can be appropriate to use θ and σ_1, assuming that is the variable associated to the most contractive fiber of the isochronous leave.
- The parameterization method extends to other invariant objects, so that we can think on higher dimensional objects (tori,...) that can naturally appear as attractors in small networks.

Conclusions, remarks and future work II

- Impact of input noise on PRFs compared to PRCs or relevance of transient effects for noisy stimuli? Extension of the concept to stochastic processes? Experimental tests of our theoretical findings?
- Experimental tests: we aim at showing the relevance in situations with realistic synaptic “bombardment". Questions: how to measure the PRFs and the ARFs? Use generalized stimulation protocols? Link to [Galán et al], [Canavier et al]?

Thanks for your attention

Funding agencies:

AGAUR Agència de Gestió d'Ajuts Universitaris i de Recerca

2014-SGR-504

GOBIERNO DE ESPAÑA MINISTERIO DE ECONOMÍA Y COMPETITIVIDAD

MTM2015-65715-P, MTM2015-71509-C2-2-R, RyC-...

Examples 1 and 2: iterates

Iterates (1000) for an equidistant grid (θ, x-axis and x, y-axis) for the full map $r = 0.1$, $\varepsilon = 0.001$ and $\gamma = 0.08$ (left) and $\gamma = 0.008$ (right), and the last iterate for each initial condition (iterate number 1000 (left) or 1000000 (right)) in black. Colors indicate the section $s = 1$ or $s = -1$.

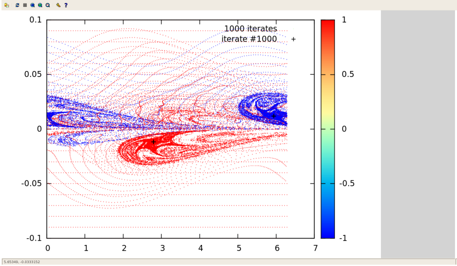

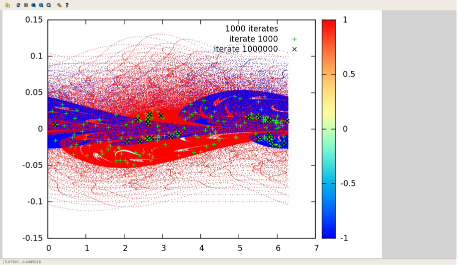

Examples 1 and 2: iterates

Iterates (5000) for initial conditions of $x = -0.1$, $\theta_0 = \theta_1 = 0$ (θ_0, x-axis and θ_1, y-axis, x_n, z-axis) for the full map $r = 0.1$, $\varepsilon = 0.001$ and $\gamma = 0.08$ (left) and $\gamma = 0.008$ (right), and the last iterate for each initial condition on an equidistant grid (iterate number 5000). Colors indicate the section $s = 1$ or $s = -1$.

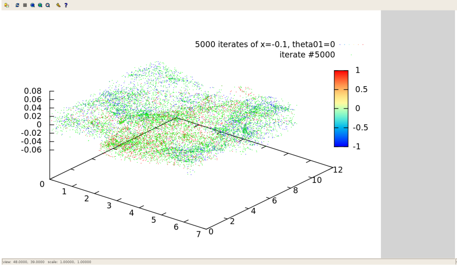

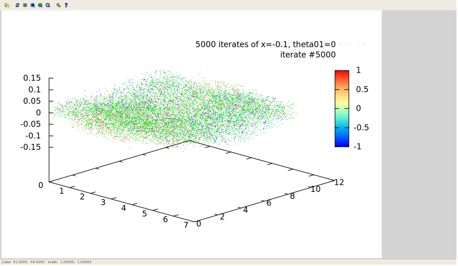

Examples 1 and 2: spectrograms

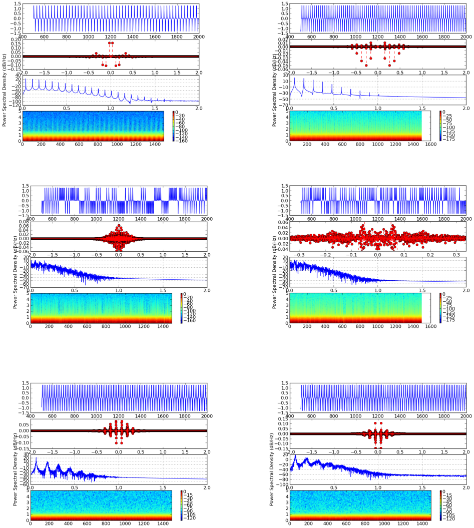

Time series, Fourier coefficients and PSD for initial conditions of $x = 0.1$, $y = 0.1$, $\theta_i = 0$ for $\gamma = 0.08$ and: (L1) $\varepsilon = 0$; (R1) $\varepsilon = 0.001$, $\omega_1 = 1$; (L2) $\varepsilon = 0.001$, $\omega_1 = 1$ and $\omega_2 = (\sqrt{5} - 1)/2$; (R2) $\varepsilon = 0.001$, $\omega_1 = 1$, $\omega_2 = (\sqrt{5} - 1)/2$ and $\omega_3 = \Omega^2$. (L3) Noise injected to (x, y)-system, only to y-variable $\varepsilon = 0.001$. (R3) Noise injected to (u, v)-system, to both variables $\varepsilon = 0.001$

Examples 1 and 2: spectrograms

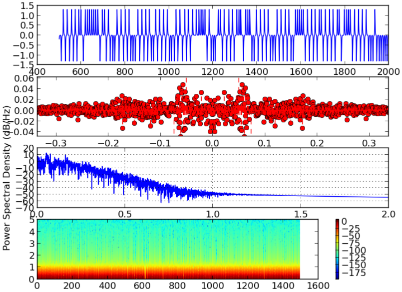

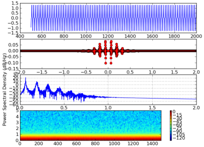

Duffing equation: Time series, Fourier coefficients and PSD for initial conditions of $x = 0.1$, $y = 0.1$, $\theta_i = 0$ for $\gamma = 0.08$. (L) $\varepsilon = 0.001$, $\omega_1 = 1$, $\omega_2 = (\sqrt{5} - 1)/2$ and $\omega_3 = \Omega^2$. (R) Noise injected to (x, y)-system, only to y-variable, $\varepsilon = 0.001$.

Examples 1 and 2: spectrograms

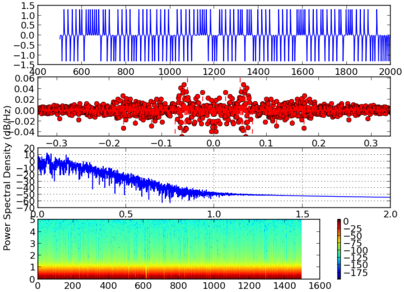

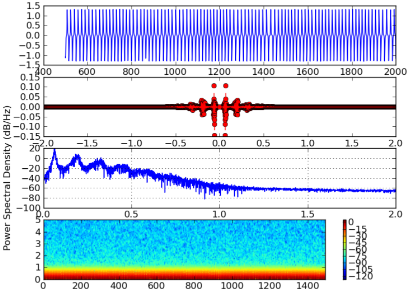

Duffing equation: Time series, Fourier coefficients and PSD for initial conditions of $x = 0.1$, $y = 0.1$, $\theta_i = 0$ for $\gamma = 0.08$. (L) $\varepsilon = 0.001$, $\omega_1 = 1$, $\omega_2 = (\sqrt{5} - 1)/2$ and $\omega_3 = \Omega^2$. (R) Noise injected to (x, y)-system, to both variables $\varepsilon = 0.001$.

SM: approximate expression for the local map components

$$L^+ : H^+_{in} \longrightarrow H^+_{out}$$

$$\begin{aligned}
x_1 &= r_x \left(\frac{r_y}{y_0}\right)^{-(1-l_x)/l_y}, \\
\theta_1 &= \theta_0 + \omega \frac{1}{l_y} \ln \frac{r_y}{y_0}, \\
G_1 &= F_0 \psi^2 - 2\, r_x (\psi^2 - 1) + 2 \left(-1 + \sqrt{1 + F_0 - 2\, r_x^2}\right) \psi (1 - \psi),
\end{aligned}$$

with $\psi := \left(\frac{r_y}{y_0}\right)^{-2/l_y}$, $x = r_x$ and $y = r_y$ define H^+_{in} and H^+_{out}, resp.

Similar expression for $L^- : H^-_{in} \longrightarrow H^-_{out}$.

SM: approximate expression for the global map components I

$$T_G^{\pm} : H_{out}^{+} \longrightarrow H_{in}^{-}$$

- Both G and x satisfy linear differential equations in G and x, respectively.

$$\dot{G} = -a\,G + b, \qquad \dot{x} = c\,G + d,$$
$$a := 2(p^2 + x^2 + y^2), \qquad b := -2x^2(1-p) + 4I_y y^2 + 4\eta_y y,$$
$$c := [(0.5-p)(p+1) - x^2 - y^2], \qquad d := I_x x + \eta_x.$$

- Solving the differential equations from time $t = T_1$ on H_{out}^{+} to $t = T_2$ on H_{in}^{-}, we get expressions like:

$$G(T_2) = G(T_1)\exp\left(-\int_{T_1}^{T_2} a(s)\,ds\right) + \int_{T_1}^{T_2} b(t)\left(\exp\int_{T_2}^{t} a(s)\,ds\right)\,dt$$

SM: approximate expression for the global map components II

- We approximate the solutions by integrating the differential equations on the unperturbed heteroclinic orbit $S_{\pm}$ (analogous to variational equations).
- Finally, we get:

$$\begin{aligned} G_2 &= \alpha\, G_1 + f(\theta; I_x, \epsilon) \\ x_2 &= \hat{\alpha}\, x_1 + \hat{f}(\theta; I_x, \epsilon) \\ \theta_2 &= \theta_1 + \omega\,(T_2 - T_1). \end{aligned}$$

- α, $\hat{\alpha}$, f and $\hat{f}$ are computed from the differential equations for G and x. For the functions f and $\hat{f}$, we integrate for different initial conditions of θ_1 and then Fourier-transform.
- All the procedure is done once and the model remains then fixed.

Similar expression for $T_G^{\mp} : H_{out}^{-} \longrightarrow H_{in}^{+}$.